

Electromagnetic Modeling of a Waveguide-Based Strip-to-Slot Transition Module for Application to Spatial Power Combining Systems

A.B. Yakovlev^{*1}, A.I. Khalil¹, C.W. Hicks¹, M.B. Steer²

¹Department of Electrical and Computer Engineering

North Carolina State University, Raleigh, North Carolina 27695-7914, USA

²Institute of Microwaves and Photonics, School of Electronic and Electrical Engineering, University of Leeds, Leeds, LS2 9JT, United Kingdom

Abstract

A method of moments integral equation formulation is proposed for the full-wave analysis of an arbitrarily shaped waveguide-based strip-to-slot transition module for application to spatial power combining systems. A Generalized Scattering Matrix (GSM) of the transition is obtained as an individual GSM in the cascading algorithm for a composite GSM of power combining systems. The proposed approach can be efficiently used in modeling electrically thin substrates rather than individual GSM cascading of individual electric and/or magnetic layers.

Introduction

The development of waveguide-based spatial power combining systems [1,2] requires full-wave electromagnetic modeling of waveguide-based passive circuit elements, and application of field-circuit interaction techniques to handle interaction between passive and active (MMIC) devices and circuits. A novel Method of Moments (MoM)-based GSM modeling scheme has been recently proposed to efficiently simulate large electromagnetic and quasi-optical systems in rectangular waveguide[3]. A whole system is partitioned into modules each of which is an electric or magnetic layer. A full-wave MoM formulation of an individual layer is provided resulting in a GSM of each layer. A length of waveguide is separately modeled as a diagonal GSM with elements being the propagation factor of each waveguide mode. Internal ports connecting MMIC devices and passive circuit elements with the distributed structure are also incorporated in the cascading algorithm. The GSM is constructed for all propagating and evanescent TE and TM modes and provides an accurate simulation of interactions between neighboring modules. A problem occurs when the separation between neighboring layers becomes electrically small. Then the number of waveguide modes, i.e. the size of the GSM, must increase significantly. This greatly increases memory and computational requirements.

In this paper we propose a full-wave electromagnetic modeling of a strip-to-slot transition module for the accurate analysis of thin substrates (separation between electric and magnetic layers). In essence the MoM-based GSM formulation is developed for two close layers which is then modeled as a single module. Electric field and magnetic field integral equation formulations are discretized via MoM are obtained resulting in the GSM for the transition. The method is numerically stable for thin as well as thick substrates and does not require additional computational efforts for varying separation between electric and magnetic layers. Numerical results are obtained for a rectangular strip-to-slot transition in waveguide and compared with those generated by a commercial FEM program.

Theory

Consider the strip-to-slot transition module with three dielectric layers in a rectangular waveguide shown in Fig. 1. An arbitrarily shaped metallization S_m (electric layer) and slot apertures S_s in a ground plane are located on the interfaces of adjacent dielectric layers with permittivities ϵ_1 and ϵ_2 , and ϵ_2 and ϵ_3 , respectively. The

0-7803-5639-X/99/\$10.00 ©1999 IEEE.

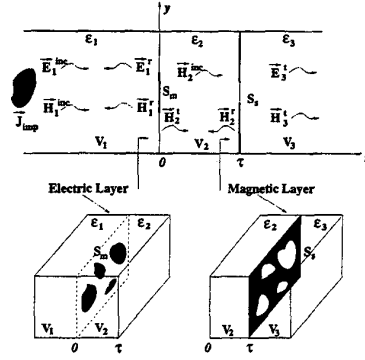


Figure 1: Geometry of a waveguide-based arbitrarily shaped strip-to-slot transition module.

incident electric and magnetic fields in the region V_1 are generated by an impressed electric current source \vec{J}_{imp} (an incident magnetic field from region V_3 is similarly handled).

The electric field integral equation formulation for the unknown electric current density $\vec{J}(\vec{r}')$ and magnetic current density $\vec{M}(\vec{r}')$ is obtained enforcing the boundary condition on the tangential components of the electric field on the conducting surface S_m at $z = 0$:

$$\begin{aligned} \hat{z} \times \vec{E}_1^{inc}(\vec{r}) &= j\omega\mu_0 \hat{z} \times \int_{S_m} \vec{J}(\vec{r}') \cdot \vec{G}_{e1}^{(11)}(\vec{r}', \vec{r}) dS' - \\ &- \hat{z} \times \int_{S_a} \vec{M}(\vec{r}') \cdot [\nabla' \times \vec{G}_{e1}^{(21)}(\vec{r}', \vec{r})] dS'. \end{aligned} \quad (1)$$

Here the integrals on the right side of (1) represent the scattered electric field due to induced electric $\vec{J}(\vec{r}')$ and magnetic $\vec{M}(\vec{r}')$ currents. The electric dyadic Green's functions $\vec{G}_{e1}^{(11)}(\vec{r}, \vec{r}')$, $\vec{G}_{e1}^{(21)}(\vec{r}, \vec{r}')$ are obtained as the solution of the boundary-value problem for a semi-infinite two-layered waveguide terminated with a ground plane at $z = \tau$ (similar formulations for electric Green's dyadics are presented in [4]). The electric dyadic Green's functions satisfy boundary and continuity conditions for the electric field vector on the surface of a conducting shield and on the interface of adjacent dielectric layers with permittivities ϵ_1 and ϵ_2 .

The continuity condition for tangential components of the magnetic field on the surface of the aperture S_a at $z = \tau$ results in the magnetic field integral equation for the unknown currents $\vec{J}(\vec{r}')$ and $\vec{M}(\vec{r}')$:

$$\begin{aligned} \hat{z} \times \vec{H}_2^{inc}(\vec{r}) &= -\frac{\epsilon_2}{\epsilon_1} \hat{z} \times \int_{S_m} \vec{J}(\vec{r}') \cdot [\nabla' \times \vec{G}_{e2}^{(12)}(\vec{r}', \vec{r})] dS' - \\ &- j\omega\epsilon_0 \hat{z} \times \int_{S_a} \vec{M}(\vec{r}') \cdot [\epsilon_2 \vec{G}_{e2}^{(22)}(\vec{r}', \vec{r}) + \epsilon_3 \vec{G}_{e3}(\vec{r}', \vec{r})] dS' \end{aligned} \quad (2)$$

where the integrals on the right side of (2) represent the scattered magnetic field due to induced electric $\vec{J}(\vec{r}')$ and magnetic $\vec{M}(\vec{r}')$ currents. Note that the incident

magnetic field $\vec{H}_2^{inc}(\vec{r})$ is part of an incident magnetic field generated in the region V_1 and transmitted through the dielectric interface at $z = 0$. The electric dyadic Green's functions $\vec{G}_{e2}^{(12)}(\vec{r}, \vec{r}')$, $\vec{G}_{e2}^{(22)}(\vec{r}, \vec{r}')$ have been derived for semi-infinite two-layered waveguide satisfying boundary and continuity conditions for the magnetic field vector. The electric dyadic Green's function $\vec{G}_3(\vec{r}, \vec{r}')$ is obtained for a single-layered semi-infinite waveguide terminated with a ground plane at $z = \tau$. Green's functions in this formulation are obtained in terms of double series expansions over the complete system of eigenfunctions of the Helmholtz operator.

The incident electric and magnetic fields are expressed in terms of eigenmode expansions with unknown magnitudes, including both propagating and evanescent TE and TM modes normalized by a unity power condition [5]. The coupled set of integral equations (1), (2) is discretized via the MoM using rectangular cells on the strip S_m and slot S_s surfaces with the x - and y -directed piecewise sinusoidal basis and testing functions for $\vec{J}(\vec{r}')$ and $\vec{M}(\vec{r}')$ currents. The MoM matrix equation yields a matrix representation for the electric and magnetic current amplitude coefficients in terms of the unknown magnitudes of incident electric and magnetic fields (eigenmode expansions) and the inverse MoM matrix. The magnitudes of scattered (reflected and transmitted) modes are obtained in terms of current amplitude coefficients using a unity power normalization for the electric and magnetic vector functions. Finally, this procedure results in the GSM representation relating magnitudes of incident and scattered modes (similar matrix approach is described in [3] for a single electric layer).

Results and Discussion

Numerical results are obtained for the example of a rectangular strip-to-slot transition module (geometry shown in Fig. 2) and compared with those generated by the HFSS (Hewlett Packard, version 5.2). Fig.'s 3-6 demonstrate dispersion characteristics (magnitude and phase) for the reflection S_{11} and transmission S_{21} coefficients in a narrow resonance frequency range (18.5-20.4 GHz) for the dominant TE_{10} mode. Very good agreement between the MoM numerical solution and the HFSS results is observed. Fig. 7 shows the behavior of the transmission S_{21} coefficient (magnitude) versus separation τ between the strip metallization and slot aperture. The results are obtained at the frequency 19.635 GHz (resonance frequency demonstrated in Fig.'s 3-6 for $\tau=2.5$ mm). It can be seen that the structure resonates at the same frequency for different distances between strip and slot. The algorithm is numerically stable for different material and geometrical parameters, including thin substrates with a high dielectric permittivity, and it does not require additional CPU time and memory.

Acknowledgments

This work was supported by the U.S. Army Research Office through Clemson University as a Multidisciplinary University Research Initiative on Quasi-Optical Power Combining, Agreement Number DAAG55-97-K-0132.

References

- [1]. *Active and Quasi-Optical Arrays for Solid-State Power Combining*, Edited by R. York and Z. Popović. New York, NY: John Wiley & Sons, 1997.
- [2]. *Active Antennas and Quasi-Optical Arrays*. Edited by A. Mortazawi, T. Itoh and J. Harvey. New York, NY: IEEE Press, 1999.
- [3]. A. I. Khalil and M. B. Steer, "A Generalized Scattering Matrix method using the method of moments for electromagnetic analysis of multilayered structures in waveguide," *IEEE Trans. Microwave Theory Tech.*, (to be published).
- [4]. C.-T. Tai, *Dyadic Green's Functions in Electromagnetic Theory*, IEEE Press, NJ, 1993.
- [5]. R. E. Collin, *Field Theory of Guided Waves*, IEEE Press, New York, 1991.

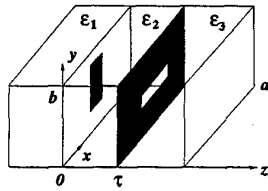


Fig. 2. Geometry of a rectangular waveguide-based strip-to-slot transition module: strip is $0.6 \text{ mm} \times 5.4 \text{ mm}$, slot is $5.4 \text{ mm} \times 0.6 \text{ mm}$, $a = 22.86 \text{ mm}$, $b = 10.16 \text{ mm}$, $r = 2.5 \text{ mm}$, $\epsilon_1 = 1.0$, $\epsilon_2 = 6.0$, $\epsilon_3 = 1.0$.

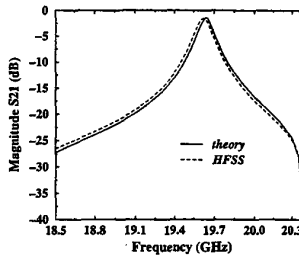


Fig. 5. Magnitude of the transmission coefficient S_{21} against frequency.

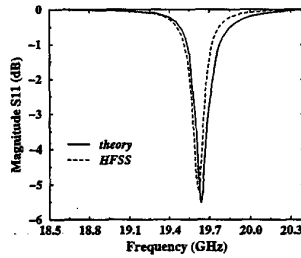


Fig. 3. Magnitude of the reflection coefficient S_{11} against frequency.

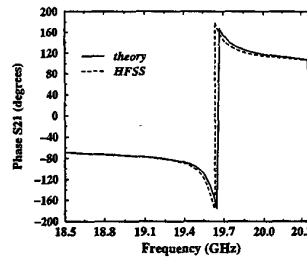


Fig. 6. Phase of the transmission coefficient S_{21} against frequency.

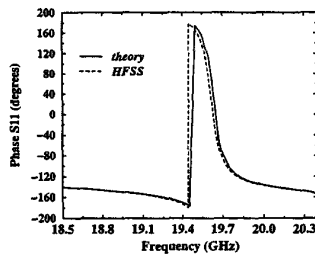


Fig. 4. Phase of the reflection coefficient S_{11} against frequency.

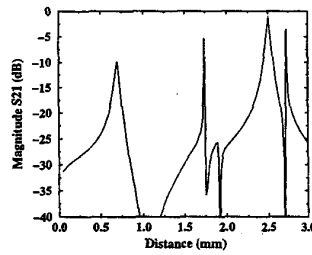


Fig. 7. Magnitude of the transmission coefficient S_{21} against separation r between strip and slot.